International Journal of Applied Mathematics and Engineering Sciences
Vol. 2 No. 2 (December, 2017)

BOUNDARY ELEMENT FORMULATION FOR FLOW IN UNSATURATED POROUS MEDIA

Bruno Natalini, Viktor Popov & Carlos A. Brebbia

ABSTRACT: Numerical model for two phase (air and water) unsaturated flow has been derived and solved using the boundary element method (BEM). The equations have been represented as non-homogeneous Laplace equations, and the non-homogeneous part has been dealt with by using the dual reciprocity method (DRM). The soil-water characteristic curve according to the modified van Genuchten approach was employed. The developed scheme was applied to solution of upward and downward infiltration in clay showing good agreement with numerical solutions previously reported in open literature.

1. INTRODUCTION

Modelling of unsaturated flow in porous media is applied in a number of different areas. Some areas of interest include hydrology, environmental protection and remediation and disposal of hazardous waste in underground repositories. In this work a numerical model for unsaturated flow where both phases, water and air, are modelled is developed. Such model could be of importance for solution of the problem of wetting of clay in underground repositories where the air cannot escape freely during the wetting of the clay, a process which may increase the air pressure slowing down the actual wetting process.

The model is solved by using the BEM DRM-MD approach which has shown good stability for solving non-linear problems in the past.

2. GOVERNING EQUATIONS FOR FLOW IN UNSATURATED POROUS MEDIA

In this section a quick derivation of the governing equations is presented. It is considered that each phase occupies part of the domain and follows its own set of tortuous paths. A detailed treatment of the theory of flow in unsaturated media is given by Bear & Verruijt [1] and Helmig [2].

2.1 Equation for the water phase

The mass balance equation is given as

$$\frac{\partial\left(n\rho_w S_w\right)}{\partial t} + \vec{\nabla}\cdot\rho_w\vec{q}_w = 0 \tag{1}$$

where:

n is the porosity

ρ_w is the water density

S_w is the water saturation

S_w is defined as the relation of the volume of water in a representative elementary volume (REV) and the volume of voids in the REV. S_w ranges from zero to one.

The specific discharge is defined using the Darcy law

$$\vec{q}_w = -\frac{k_w}{\mu_w}\left(\vec{\nabla}p_w - \rho_w g\vec{\nabla}z\right) \tag{2}$$

where:

k_w is the effective permeability for water (a function of S_w)

m_w is the dynamic viscosity of water

p_w is the water pressure

z is the elevation

By substituting (2) into (1) and considering that n and r_w are constant, (1) can take the following form

$$\nabla^2 p_w = \frac{\mu_w}{k_w} n \frac{\partial S_w}{\partial t} - \frac{1}{k_w} \vec{\nabla} k_w \cdot \vec{\nabla} p_w + \frac{\rho_w g}{k_w} \vec{\nabla} k_w \cdot \vec{\nabla} z \tag{3}$$

The water relative permeability is defined as

$$k_{rw}(S_w) = \frac{k_w(S_w)}{k_w(1)} \tag{4}$$

and

$$k_w(1) = \frac{\mu_w K_w}{\rho_w g} \tag{5}$$

where K_w is the hydraulic conductivity for water, yielding

$$k_w(S_w) = \frac{k_{rw}(S_w) K_w \mu_w}{\rho_w g} \tag{6}$$

By substituting (6) into (3), the equation for the water phase is obtained as

$$\nabla^2 p_w = \frac{n\rho_w g}{k_{rw} K_w} \frac{\partial S_w}{\partial t} - \frac{1}{k_{rw}} \vec{\nabla} k_{rw} \cdot \vec{\nabla} p_w + \frac{\rho_w g}{k_{rw}} \vec{\nabla} k_{rw} \cdot \vec{\nabla} z \tag{7}$$

Note that it is possible to use equation (3) for the water phase, however (7) is a more suitable form since k_{rw} is non-dimensional and ranges from 0 to 1. Conversely, k_w has dimensions, which makes its order of magnitude dependant on the scale factors, which can produce higher errors when the term $\frac{1}{k_w} \nabla k_w$ is calculated rather than $\frac{1}{k_{rw}} \nabla k_{rw}$.

2.2 Equation for the Air Phase

The starting point for development of the equation for air phase is the mass balance equation:

$$\frac{\partial (n \rho_a S_a)}{\partial t} + \vec{\nabla} \cdot \rho_a \vec{q}_a = 0 \tag{8}$$

combined with the Darcy law

$$\vec{q}_a = -\frac{k_a}{\mu_a}\left(\vec{\nabla} p_a - \rho_a g \vec{\nabla} z\right) \tag{9}$$

where the nomenclature analogous to the one in (1) and (2), the sub-index '*a*' identifying air properties. Note that

$$S_w + S_a = 1 \tag{10}$$

By substituting (9) into (8), considering *n* to be constant and neglecting the gravitational term $\rho_a g \vec{\nabla} z$, and by using $\frac{k_a}{\mu_a} = \frac{k_{ra} K_a}{\rho_a g}$, the following equation is obtained

$$n\frac{\partial(\rho_a S_a)}{\partial t} - \frac{K_a}{g}\vec{\nabla}\cdot\left(k_{ra}\vec{\nabla} p_a\right) = 0 \tag{11}$$

Further, developing both terms in (11), considering that r_a is linked to p_a through the equation of state and rearranging the equation yields

$$\nabla^2 p_a = \frac{g}{k_{ra} K_a}\left[\frac{n}{R'T}\left(S_a\frac{\partial p_a}{\partial t} + p_a\frac{\partial S_a}{\partial t}\right) - \frac{K_a}{g}\left(\vec{\nabla} k_{ra}\cdot\vec{\nabla} p_a\right)\right] \tag{12}$$

The derivative in time of the saturation appearing in (7) and (12) can be handled in the following way:

$$\frac{\partial S_w}{\partial t} = \frac{dS_w}{dp_c}\frac{\partial p_c}{\partial t} = \frac{dS_w}{dp_c}\frac{\partial p_c}{\partial p_\gamma}\frac{\partial p_\gamma}{\partial t} \tag{13}$$

where subscript γ stands for "*w*" or "*a*" depending on the equation that is solved. Taking into account that the capillary pressure can be expressed as $p_c = p_a - p_w$, it is obvious that $\partial p_c/\partial p_g = (1 \text{ or } -1)$. If furthermore we use (10) to eliminate S_a, the final equations for water and air become

$$\nabla^2 p_w = -\frac{n\rho_w g}{k_{rw} K_w}\frac{\partial S_w}{\partial p_c}\frac{\partial p_w}{\partial t} - \frac{1}{k_{rw}}\vec{\nabla} k_{rw}\cdot\vec{\nabla} p_w + \frac{\rho_w g}{k_{rw}}\vec{\nabla} k_{rw}\cdot\vec{\nabla} z \tag{14}$$

and

$$\nabla^2 p_a = \frac{g}{k_{ra} K_a}\left[\frac{n}{R'T}\left(\left(1 - S_w\right) - p_a\frac{\partial S_w}{\partial p_c}\right)\frac{\partial p_a}{\partial t} - \frac{K_a}{g}\left(\vec{\nabla} k_{ra}\cdot\vec{\nabla} p_a\right)\right] \tag{15}$$

Equations (14) and (15) are the equations to be solved by the code, being p_w and p_a the unknown potential fields. The constants needed in the model are g, ρ_w, n, K_w, K_a, R' and T while k_{rw}, S_w and k_{ra} are functions of p_w and p_a. The functions linking the potential fields and k_{rw}, S_w and k_{ra} variables are given by the soil water retention curve.

3. SOIL WATER RETENTION CURVE

The soil water retention curve describes the relation between the capillary pressure, p_c, and S_w. There are several functions that have been proposed; among the most popular for the air-water system are those given by Leverett

[3], Brooks and Corey [4] and van Genuchten [5]. Recently Vogel et al. [6, 7] suggested the use of the following relation:

$$S_w = \begin{cases} S_{w0} + \dfrac{S_m - S_{w0} - S_{a0}}{\left(1 + (\mathrm{a}p_c)^{\mathrm{n}}\right)^{\mathrm{m}}} & \textit{when} \quad p_c > p_s \\ 1 & \textit{when} \quad p_c \le p_s \end{cases} \tag{16}$$

where S_m is a fictitious extrapolated parameter; $S_m > 1$, and p_s is called the minimum capillary pressure. The modified Van Genuchten's relative water permeabilities as a function of saturations are

$$k_{rw} = \sqrt{S_e}\left(\frac{1 - F(S_e)}{1 - F(1)}\right)^2 \text{ and } k_{ra} = (1 - S_e)^{\frac{1}{2}}\left(\frac{F(S_e) - F(1)}{1 - F(1)}\right)^2 \tag{17}$$

where

$$F(S_e) = \left(1 - S_e^{*1/\mathrm{m}}\right)^{\mathrm{m}} \text{ and } \quad S_e^* = \frac{1 - S_{w0}}{S_m - S_{w0} - S_{a0}} S_e \tag{18}$$

and

$$S_e = \frac{S_w - S_{w0}}{1 - S_{w0} - S_{a0}} \tag{19}$$

Equation (16) has been originally proposed in terms of water contents; here it is modified in order to match with the definition (19), which takes into account S_{a0}, and the relative permeability of the air phase. Equations (16) – (19) will be referred to as the modified Van Genuchten model (VGM). The modified VGM eliminates numerical instabilities appearing near saturation and this formulation is further used in the numerical examples in section 6.

4. SOLVING THE SYSTEM OF EQUATIONS

When considering the simultaneous flow of both the water and the air in the unsaturated zone, the system of equations is represented by (14) and (15) together with those coming from the soil water model. Though the numerical model is developed for the case of variable air pressure, further in this work the air pressure is considered to be constant and equal to the atmospheric pressure. Therefore, in the examples presented here only (14) is solved; which is equivalent to solving the Richard´s equation.

The code developed obtains solutions at different timesteps by using a linear time finite difference approximation. As the equations are non-linear, in each timestep an iterative procedure is applied. The code starts by calculating p_c from the initial conditions of the problem, then S_w and k_{rw} are calculated and finally (14) is solved. In the next iteration, with the obtained value of p_w, a new value for p_c is calculated, then S_w and k_{rw} are recalculated and (14) is solved again. The process is repeated until convergence is reached within each timestep.

The derivative of S_w in respect to p_c appearing in the equations will depend on the soil water retention model used and for the modified VGM it can be obtained as

$$\frac{\partial S_w}{\partial p_c} = \begin{cases} -\dfrac{\mathrm{nma}\left(S_m - S_{w0} - S_{a0}\right)\left(\mathrm{a}p_c\right)^{\mathrm{n}-1}}{\left(1+\left(\mathrm{a}p_c\right)^{\mathrm{n}}\right)^{\mathrm{m}+1}} & \textit{when} \quad p_c > p_s \\ 0 & \textit{when} \quad p_c \le p_s \end{cases} \tag{20}$$

5. BEM DRM-MD IMPLEMENTATION FOR THE WATER PHASE

The dual reciprocity method (DRM), which was introduced by Nardini & Brebbia [8], is acknowledged to be one of the most effective boundary element method (BEM) techniques for transforming domain integrals into boundary integrals.

Popov and Power implemented a scheme using domain subdivision in conjunction with the DRM to avoid domain integration and called it the Dual Reciprocity Method - Multi-Domain approach (DRM-MD). The initial problem solved using this formulation was the flow of a mixture of gases through a porous media [9, 10, 11]. The DRM-MD has also been applied to linear and non-linear advection-diffusion problems [12], driven cavity flow of Navier-Stokes equations [13], non-Newtonian fluids [14], and flow of polymers inside mixers with complex geometries [15]. Though the above applications are two-dimensional (2D), recently the technique has been applied to three-dimensional (3D) problems by Natalini and Popov [16, 17] and Peratta and Popov [18, 19].

DRM-MD does not suffer the two main problems related to standard DRM; the systems of equations produced by DRM-MD are sparse and well conditioned, and the number and position of DRM nodes is usually not critical, since small sub-domains usually require no or few interior DRM nodes.

Starting from a Poisson-like governing equation

$$\nabla^2 u\left(\boldsymbol{x},t\right) = b\left(u,\boldsymbol{x},t\right) \tag{21}$$

where $u(\boldsymbol{x},t)$ is a scalar field (potential field), $b(u,\boldsymbol{x},t)$ is the non-homogeneous term and $\boldsymbol{x}$ is a position vector in the domain with components x_i, after applying the DRM approach (for more details see Partridge *et al*. [20]), the following equation is obtained

$$\lambda(\boldsymbol{x})u(\boldsymbol{x}) + \int_\Gamma q^*(\boldsymbol{x},\boldsymbol{y})u(\boldsymbol{y})d\Gamma_y - \int_\Gamma u^*(\boldsymbol{x},\boldsymbol{y})q(\boldsymbol{y})d\Gamma_y \cong$$

$$\sum_{k=1}^{J+I}\left\{\alpha_k\left(\lambda(\boldsymbol{x})\hat{u}(\boldsymbol{x},z^k) + \int_\Gamma q^*(\boldsymbol{x},\boldsymbol{y})\hat{u}(\boldsymbol{y},z^k)d\Gamma_y - \int_\Gamma u^*(\boldsymbol{x},\boldsymbol{y})\hat{q}(\boldsymbol{y},z^k)d\Gamma_y\right)\right\} \tag{22}$$

where $u^*(\boldsymbol{x},\boldsymbol{y})$ is the fundamental solution of the Laplace equation, $q(\boldsymbol{y}) = \partial u(\boldsymbol{y})/\partial n$, $q^*(\boldsymbol{x},\boldsymbol{y}) = \partial u^*(\boldsymbol{x},\boldsymbol{y})/\partial n$ and n is the unit vector normal to the boundary of the domain. The constant $\mathrm{l}(\boldsymbol{x})$ has values between 1 and 0, being equal to 1/2 on smooth parts of boundaries and being equal to 1 for points inside the domain. Constants a_k are unknown coefficients and the DRM approximation is applied to J nodes on the boundary Γ of the domain and I nodes inside the domain W.

After application of collocation technique to all boundary nodes, (22) can be written in terms of four matrices, $\mathbf{H}$, $\mathbf{G}$, $\hat{\mathbf{U}}$ and $\hat{\mathbf{Q}}$ which depend only on the geometry of the problem.

$$\mathbf{H}\boldsymbol{u} - \mathbf{G}\boldsymbol{q} = (\mathbf{H}\hat{\mathbf{U}} - \mathbf{G}\hat{\mathbf{Q}})\boldsymbol{\alpha} \tag{23}$$

Since the non-homogeneous term $\boldsymbol{b}$ in the DRM is expressed in the following form

$$\boldsymbol{b} = \mathbf{F}\boldsymbol{\alpha} \tag{24}$$

after expressing $\boldsymbol{a}$ in terms of $\boldsymbol{b}$, the following equation is obtained

$$\mathbf{H}\boldsymbol{u} - \mathbf{G}\boldsymbol{q} = (\mathbf{H}\hat{\mathbf{U}} - \mathbf{G}\hat{\mathbf{Q}})\mathbf{F}^{-1}\boldsymbol{b} \tag{25}$$

The DRM integral formulation for p_w is obtained by replacing the non-homogeneous term in (14) into (25)

$$\sum_{j=1}^{n} h_{ij}\, p_{w_j} - \sum_{j=1}^{n} g_{ij}\, q_{w_j} = \sum_{j=1}^{n} s_{ij} \left[\begin{array}{l} -\dfrac{n\rho_w g}{\widetilde{k}_{rw_j} K_w} \dfrac{\partial \widetilde{S}_{w_j}}{\partial p_c} \dfrac{\partial p_{w_j}}{\partial t} - \\ \dfrac{1}{\widetilde{k}_{w_j}} \left(\dfrac{\partial \widetilde{k}_{rw_j}}{\partial x} \dfrac{\partial p_{w_j}}{\partial x} + \dfrac{\partial \widetilde{k}_{rw_j}}{\partial y} \dfrac{\partial p_{w_j}}{\partial y} + \dfrac{\partial \widetilde{k}_{rw_j}}{\partial z} \dfrac{\partial p_{w_j}}{\partial z} \right) \end{array} \right] + \sum_{j=1}^{n} s_{ij} \frac{\rho_w g}{\widetilde{k}_{rw_j}} \frac{\partial \widetilde{k}_{rw_j}}{\partial z} \tag{26}$$

where s_{ij} is the matrix $(\mathbf{H}\hat{\mathbf{U}} - \mathbf{G}\hat{\mathbf{Q}})\mathbf{F}^{-1}$ and $\widetilde{k}_{rw_j}$ and $\partial \tilde{S}_{w_j} / \partial p_c$ are calculated using values of $p_a = p_{atm}$ (atmospheric pressure) and p_w coming from the previous iteration, which will be denoted by $\widetilde{p}_w$ from here on. $\dfrac{\partial p_{w_j}}{\partial x}$ and all the others partial derivatives are obtained by applying the DRM approximation (24) which in index notation is given as

$$\frac{\partial p_{w_j}}{\partial x} = \sum_{k=1}^{n} \sum_{l=1}^{n} \frac{\partial f_{jl}}{\partial x}\, f_{lk}^{-1}\, p_{w_k} \tag{27}$$

The time discretization is based on the implicit/explicit Euler method

$$p_w = \left(1 - \theta_{p_w}\right) p_w{}^{\mathrm{m}} + \theta_{p_w}\, p_w{}^{\mathrm{m+1}} \tag{28}$$

$$q_w = \left(1 - \theta_{q_w}\right) q_w{}^{\mathrm{m}} + \theta_{q_w}\, q_w{}^{\mathrm{m+1}} \tag{29}$$

The time derivative is approximated using a finite-difference scheme

$$\frac{\partial p_w}{\partial t} = \frac{1}{\Delta t}\left(p_w{}^{\mathrm{m+1}} - p_w{}^{\mathrm{m}}\right) \tag{30}$$

By applying (27) – (30), (26) can be recast as

$$\left(\theta_{p_w}\mathbf{H} + \frac{\widetilde{\mathbf{R}}_w}{\Delta t} + \theta_{p_w}\widetilde{\mathbf{T}}\mathbf{w}\right) \boldsymbol{p}_w{}^{\mathrm{m+1}} - \theta_{q_w}\mathbf{G}\,\boldsymbol{q}_w{}^{\mathrm{m+1}} = \left[\left(\theta_{p_w} - 1\right)\left(\mathbf{H} + \widetilde{\mathbf{T}}\mathbf{w}\right) + \frac{\widetilde{\mathbf{R}}_w}{\Delta t}\right] \boldsymbol{p}_w{}^{\mathrm{m}} + \left(1 - \theta_{q_w}\right)\mathbf{G}\,\boldsymbol{q}_w{}^{\mathrm{m}} + \rho_w g\, \mathbf{S}\,\widetilde{\mathbf{v}} \tag{31}$$

where $\widetilde{\mathbf{R}}_w$ is a matrix of components

$$\widetilde{r}_{w_{ij}} = s_{ij} \frac{n\rho_w g}{\widetilde{k}_{rw_j} K_w} \frac{\partial \widetilde{S}_{w_j}}{\partial p_c} \tag{32}$$

and $\widetilde{\mathbf{T}}_{\mathbf{W}}$ is defined as

$$\tilde{\mathbf{T}}\mathbf{w} = \left(\tilde{\mathbf{D}}_x \frac{\partial \mathbf{F}}{\partial x} \mathbf{F}^{-1} + \tilde{\mathbf{D}}_y \frac{\partial \mathbf{F}}{\partial y} \mathbf{F}^{-1} + \tilde{\mathbf{D}}_z \frac{\partial \mathbf{F}}{\partial \mathrm{z}} \mathbf{F}^{-1} \right) \tag{33}$$

where $\widetilde{\mathbf{D}}_x$ has components

$$d_{ij} = s_{ij} \frac{1}{\widetilde{k}_{rw_j}} \frac{\partial \widetilde{k}_{rw_j}}{\partial x} \tag{34}$$

and similar for $\widetilde{\mathbf{D}}_y$ and $\widetilde{\mathbf{D}}_z$ matrices. The components of vector $\widetilde{\mathbf{v}}$ is defined as

$$\widetilde{v}_j = \frac{1}{\widetilde{k}_{rw_j}} \frac{\partial \widetilde{k}_{rw_j}}{\partial \mathrm{z}} \tag{35}$$

The interface conditions between two sub-domains for pressure and flux state that the pressure and the flux must preserve continuity. In the case of pressure the interface conditions result in the following equation

$$p_{w1} = p_{w2} \tag{36}$$

In the case of flux the interface conditions are equivalent to applying the mass conservation principle and can be derived starting from the flux of water trough the interface per unit surface and unit time for both interfaces as given below

$$Q_1 = \vec{q}_{w_1} \cdot \vec{\mathrm{n}}_1 \text{ and } Q_2 = \vec{q}_{w_2} \cdot \vec{\mathrm{n}}_2 \tag{37}$$

where $\vec{\mathrm{n}}_1$ and $\vec{\mathrm{n}}_2$ are the unit normal vectors to the interface calculated from Ω_1 and Ω_2 respectively. As $\vec{q}_{w_1} = \vec{q}_{w_2}$ and $\vec{\mathrm{n}}_1 = -\vec{\mathrm{n}}_2$ the following is valid

$$Q_1 = -Q_2 \tag{38}$$

Further considering that

$$Q_1 = -\frac{k_{w_1}}{\mu_w} q_{w_1} + \frac{k_{w_1}}{\mu_w} \rho_w g \, \mathrm{n}_{z_1} \text{ and } Q_2 = -\frac{k_{w_2}}{\mu_w} q_{w_2} + \frac{k_{w_2}}{\mu_w} \rho_w g \, \mathrm{n}_{z_2} \tag{39}$$

where n_{z_1} is the z-component of $\vec{\mathrm{n}}_1$ and n_{z_2} is the z-component of $\vec{\mathrm{n}}_2$. Finally, the matching condition for flux is obtained as

$$q_{w_2} = -\frac{k_{rw_1} K_{w_1}}{k_{rw_2} K_{w_2}} q_{w_1} - \frac{k_{rw_1} K_{w_1} - k_{rw_2} K_{w_2}}{k_{rw_2} K_{w_2}} \rho_w g \, \mathrm{n}_{z_2} \tag{40}$$

or

$$q_{w_2} = Aq_{w_1} - B \tag{41}$$

6. NUMERICAL EXAMPLES

All the examples presented here use discontinuous elements combined with the augmented thin plate spline function as approximation function in the DRM approximation with no internal DRM nodes.

6.1 CASE 1: Upward infiltration in clay

The first case simulates infiltration in a 1m long clay column that initially is assumed to be in equilibrium with an imposed water pressure, p_w, of zero Pa at the bottom of the column ($z = 1$). The boundary conditions were 98060 Pa of water pressure (atmospheric pressure) at the bottom of the column ($z = 1$) combined with zero flux at the top ($z = 0$), leading to upward infiltration against gravity. A numerical solution of this case using a 1D model has been presented by Vogel *et al*. [7]. The soil-water retention curve used was the modified Van Genuchten model. The same parameters were used as in the Vogel's example:

Porosity, n	0.38	
Hydraulic conductivity of water, K_w	5.56E-07 m/s or	4.8 cm/day
Irreducible water saturation, S_{w0}	0.17895	
Van Genuchten's a parameter	0.8 1/m or	0.008 1/cm
Van Genuchten's n parameter	1.09	

Conversely to Vogel's code, which used an adaptive time stepping algorithm, this code used a fixed timestep of 0.1 day. The 3D domain was a prismatic column of $0.2 \times 0.2 \times 1$ m^3. The mesh had 410 subdomains being finer in the bottom. Figure 1 presents a view of the mesh. Preliminary tests failed when a uniform mesh of 173 subdomains was used. In order to produce results equivalent to the 1D case, a zero flux boundary condition was imposed on the sides of the domain. In order to start the iterations of the non-linear loop in the first timestep, the code requires an initial guess for $\widetilde{p}_w$ different from zero within the domain, see Figure 2. For the results presented in Figure 3, the initial guess was that $\widetilde{p}_w$ was equal to the initial conditions when $z \leq 0.9$ and from

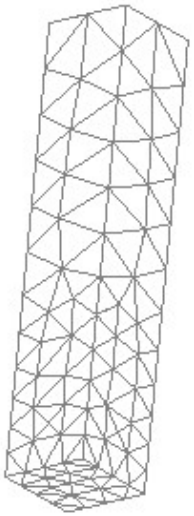

Figure 1: mesh of 410 subdomains.

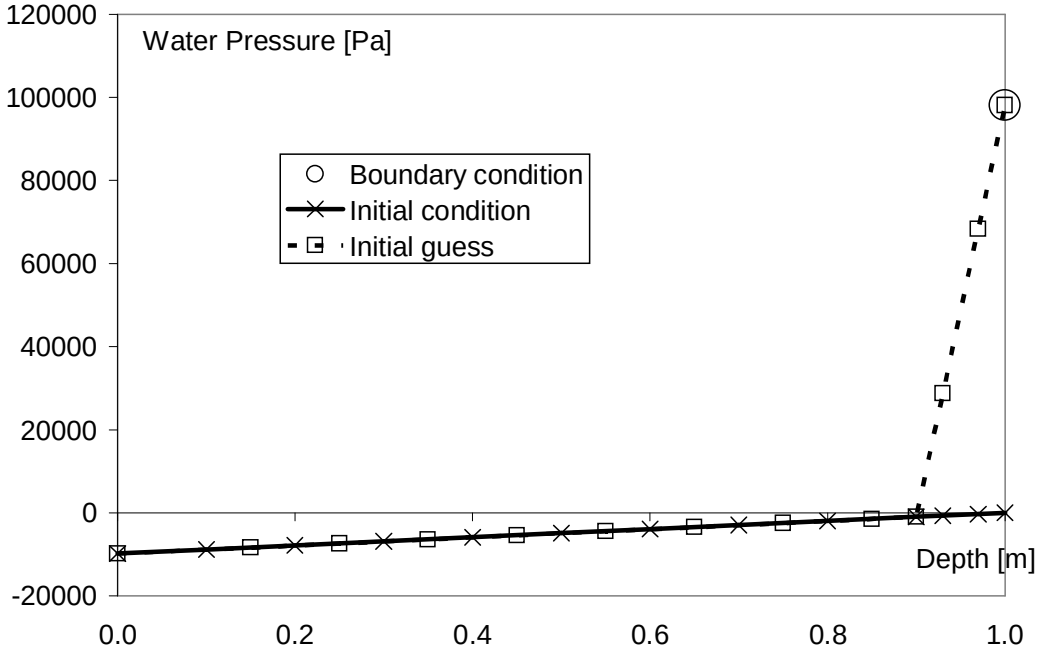

Figure 2: Initial guess and initial condition for case 1.

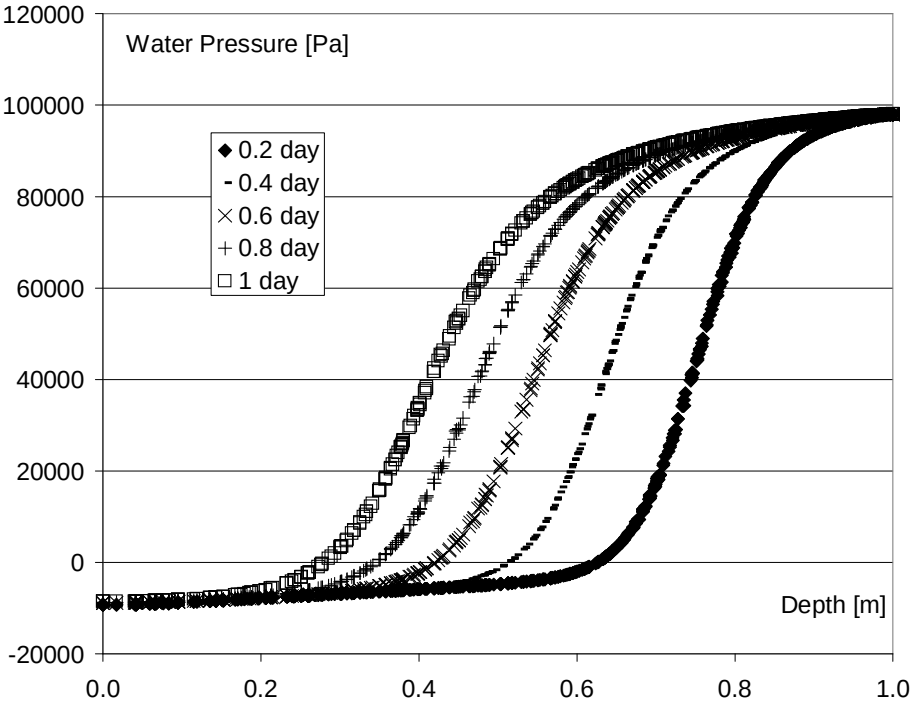

Figure 3: results of case 1

there the water pressure increased linearly up to the atmospheric pressure at $z = 1$, where it matched the boundary condition.

The agreement of the results displayed in figure 3 and those in Reference [7] is very good.

Table 1 presents the number of iterations needed in every timestep to converge. Note how the convergence is easier as the pressure distribution becomes smoother.

Table 1
Number of Iterations in Every Timestep for case 1.

Timestep	1	2	3	4	5	6	7	8	9	10
No. of iterations	19	18	15	12	11	9	8	8	6	6

6.2 CASE 2: Downward Infiltration in Clay

This example was used by Vogel *et al*. [7]. It is the simulation of infiltration in a 1m long clay column that, again, initially was assumed to be in equilibrium with an imposed water pressure, p_w, of zero Pa at the bottom of the column. The boundary conditions were 98060 Pa of water pressure (atmospheric pressure) at the top of the column combined with zero flux at the bottom, leading to downward infiltration. Three meshes were used. The first one was identical to the one displayed in Figure 1, though the domain was inverted in order to have the finer part of the mesh in the top. The other two meshes, which had 1062 and a 2233 subdomains, are shown in Figure 4. The initial guess was a linear function of the z-coordinate that started with $\widetilde{p}_w$ = atmospheric pressure at $z = 0$ (top of the domain) and decreases to meet the initial condition curve at $z = 0.1$, from there the initial guess is identical to the initial condition. Figure 5 shows the initial guess and the initial condition. The remaining part of the set up was identical to case 1.

Figures 6 to 8 show results using the three meshes described above. In Table 2 the number of iterations in every timestep is shown.

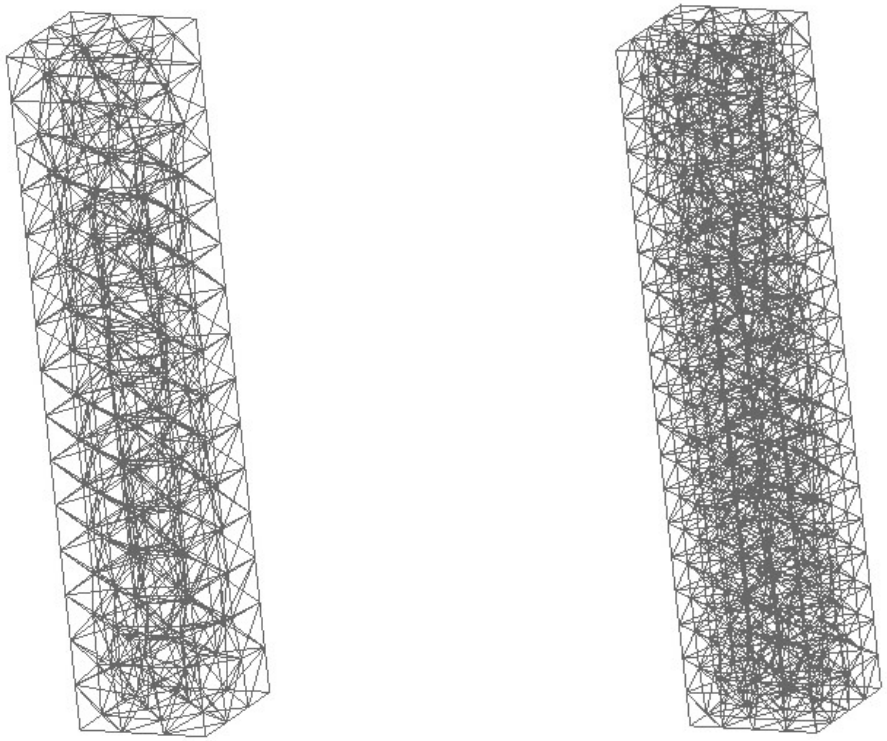

Figure 4: Case 2, View of the 1062 and 2233 Subdomains Meshes

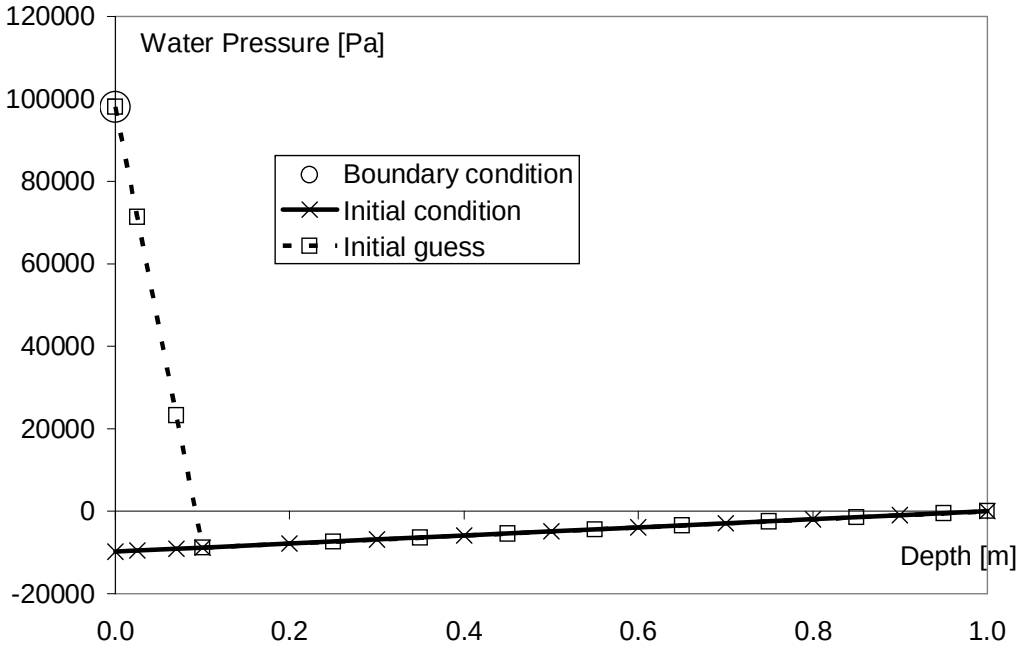

Figure 5: Initial guess and initial condition for case 2.

Solving the downward infiltration case is more difficult than the upward infiltration case because the water goes down in a sharp front that resembles a step function. The severe non-linearity of the soil-water curve near saturation makes difficult computing the term $\frac{1}{k_{rw}}\nabla k_{rw}$ in (14), because in some points near saturation there

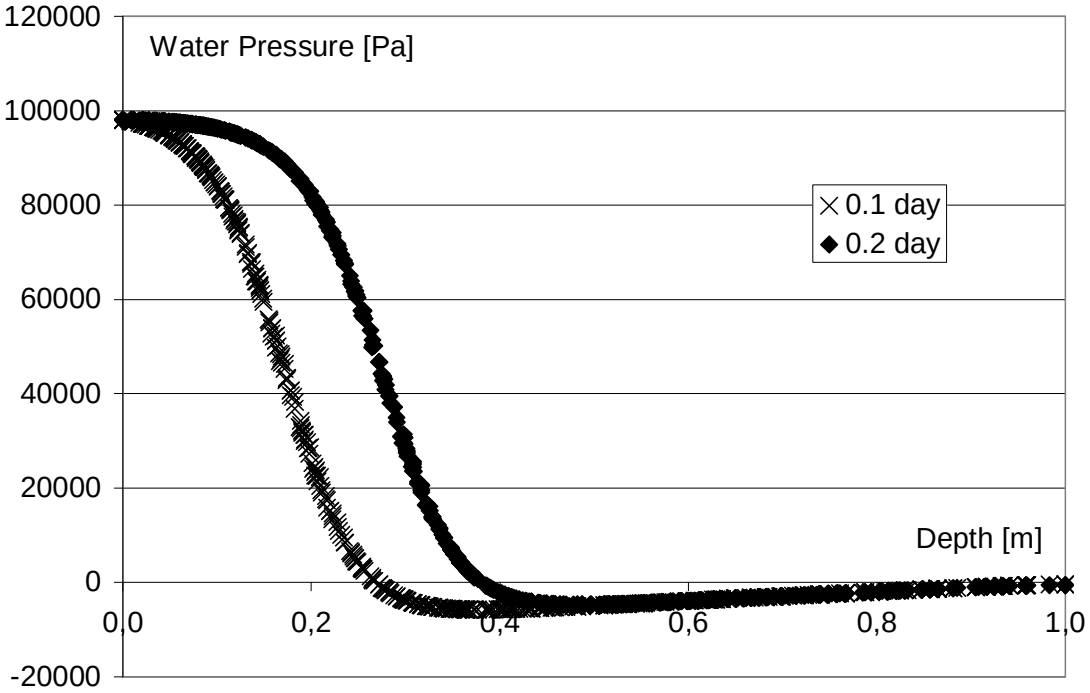

Figure 6: results of case 2 using the 410 subdomains mesh.

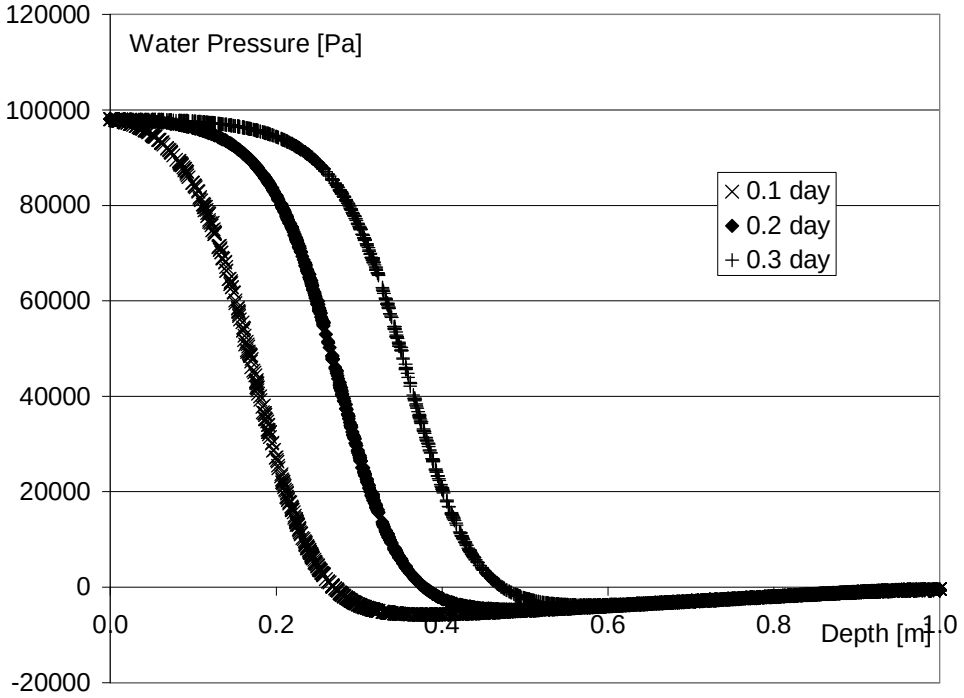

Figure 7: results of case 2 using the 1062 subdomains mesh.

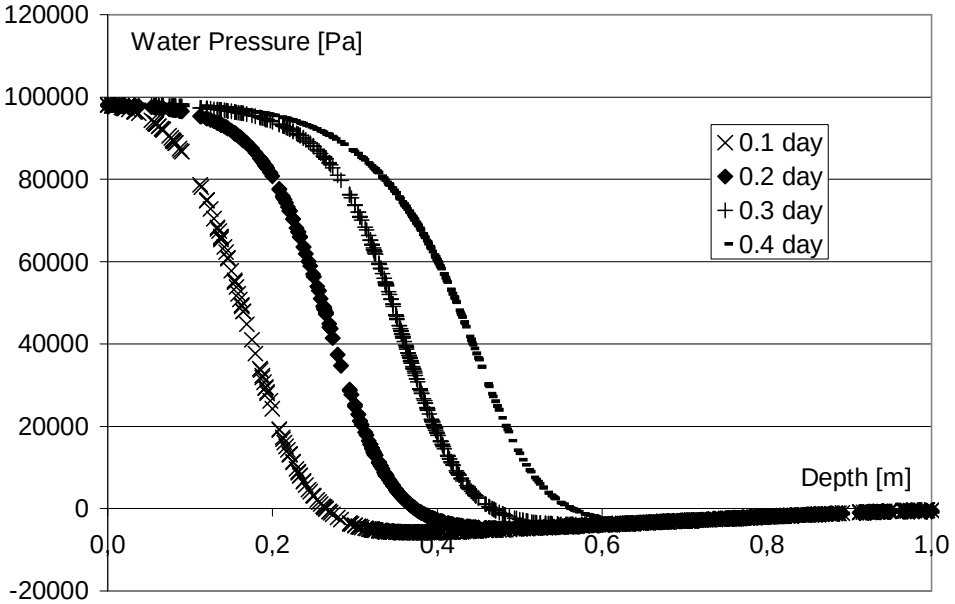

Figure 8: results of case 2 using the 2233 subdomains mesh.

are high values of ∇k_{rw} combined with very small values of k_{rw}. Compared to case 1, when using the same mesh, the code needs more iterations to converge in the first 2 timesteps (see Table 2) and it does not converge in the third timestep within 150 iterations. The code was set to stop the interative procedure after certain number of iterations (150 or 300) and these results are indicated in Table 2 as "truncated". The situation improves with mesh refinement, as can be seen in Table 2. Mesh refinement improves only the convergence; the quality of the results is similar with different meshes, provided convergence has been reached. Compared to the results of Vogel *et al.*, the agreement is not as good as in case 1.

Table 2
Number of Iterations in Every Timestep for Case 2

Timestep	*1*	*2*	*3*	*4*	*5*
410 subs	28	56	150 (truncated)	150 (truncated)	150 (truncated)
1062 subs	29	46	117	150 (truncated)	150 (truncated)
2233 subs	24	37	75	300 (truncated)	300 (truncated)

7. CONLUSIONS

Numerical model for flow in unsaturated media has been developed and solved using the BEM DRM-MD approach. The model was developed in order to predict the saturation of clay in underground repositories, which requires solving two coupled non-linear partial differential equations; one for the air and one for the water phase. Taking into account that such a complex model can be solved in different ways, in order to study the basic behaviour of the formulation under simpler conditions before solving the full two phases model, the air was assumed to be at atmospheric pressure; a situation that is equivalent to solving the Richard's equation.

The code showed that it is able to accurately solve problems of infiltration in clay. For instance, cases 1 and 2 showed an excellent performance in regard with the one-dimensional results of Vogel *et al.* [7]. However, there was slow convergence for downward infiltration. All the results indicate that the terms of the governing equation containing $\frac{1}{k_{rw}}\nabla k_{rw}$ are the cause for slower convergence in some cases. The severe non-linearity of the soil-water curve near saturation makes the task of computing the term $\frac{1}{k_{rw}}\nabla k_{rw}$ in (14) a very difficult one, because in some points near saturation there are high values of ∇k_{rw} combined with very small values of k_{rw}. The code loses accuracy when it has to calculate ∇k_{rw} and the water advances in a sharp front that resembles a step function, as it happens in case 2. Case 2 shows that the problem can be resolved by using mesh refinement. However, mesh refinement in 3D increases much more computer requirements in terms of CPU and memory than in the cases of 1D and 2D.

ACKNOWLEDGEMENT

This research was partially sponsored by the NATO Science for Peace Programme (Grant: NATO SfP 981116).

REFERENCES

[1] J. Bear and A. Verruijt, Modeling Groundwater Flow and Polution. Reidel Publishing Company, Dordrecht, Holland, 1987.

[2] Helmig, R., Multiphase Flow and Transport Processes in the Subsurface. Springer-Verlag, Berlin, 1997.

[3] Leverett, M. C., Capillary Behaviour in Porous solids. Transactions of the AIME, 142:152-169, 1941.

[4] Brooks, R. H., Corey, A. T., Hydraulic Properties of Porous Media. In Hydrol. Pap., Vol. 3, Colorado State University, Fort Collins, 1964.

[5] Van Genuchten, M. T., A Closed-form Equation for Predicting the Hydraulic Conductivity of Unsaturated Soils. Soil. Sci. Soc. Am. J., 44:892-898, 1980.

[6] Vogel, T., Cislerova, M., Reliability of Unsaturated Hydraulic Conductivity Calculated from the Moisture Retention Curve. Transport Porous Media, 1988, 3:1-15.

[7] Vogel, T., van Genuchten, M. Th., Cislerova, M., Effect of the Shape of the Soil Hydraulic Functions Near Saturation on Variably-saturated flow Predictions. Advances in Water Resurces 24 (2001) 133-144.

[8] D. Nardini and C. A. Brebbia, A New Approach to Free Vibration Analysis using Boundary Elements, *Appl. Math. Model*. **7** (1983) 157-62.

[9] V. Popov and H. Power, DRM-MD Approach for the Numerical Solution of Gas Flow in Porous Media with Application to Landfill, *Eng. Anal. Bound. Elem.*, **23** (1999) 175-88.

[10] V. Popov, H. Power and J. M. Baldasano, BEM Solution of Design of Trenches in a Multi-layered landfill, *J. Environ. Eng.–ASCE*, **124/**1 (1998) 59-66.

[11] V. Popov and H. Power, Numerical Analysis of the Efficiency of Landfill Venting Trenches, *J. Environ. Eng.–ASCE*, **126/**1 (2000) 32-38.

[12] V. Popov and H. Power, The DRM-MD Integral Equation Method: An Efficient Approach for the Numerical Solution of Domain Dominant Problems, *Int. J. Numer. Meth. Eng.*, **44** (1999) 327-353.

[13] W. F. Florez, H. Power, DRM Multidomain Mass Conservative Interpolation Approach for the BEM Solution of the Two-Dimensional Navier-Stokes equations, *Comput. Math. Appl.*, 43/3-5 (2002) 457-472.

[14] W. F. Florez, H. Power, Multi-Domain Mass Conservative Dual Reciprocity Method for the Solution of the Non-Newtonian Stokes Equations, *Appl. Math. Model*., 26/3 (2002) 397-419.

[15] W. F. Florez, *Nonlinear Flow using Dual Reciprocity*, WIT Press, Southampton, 2001.

[16] B. Natalini and V. Popov, Tests of Radial Basis Functions in the 3D DRM-MD, *Communications for Numerical Methods in Engineering*, **22** (2006) 13-22.

[17] B. Natalini and V. Popov, On the Optimal Implementation of the Boundary Element Dual Reciprocity Method – Multi Domain Approach for 3D Problems. *Engineering Analysis with Boundary Elements*, in press.

[18] A. Peratta and V. Popov, A New Scheme for Numerical Modelling of Flow and Transport Processes in 3D Fractured Porous Media, *Advances in Water Resources*, 29 (2006) 42-61.

[19] A. Peratta and V. Popov, Hybrid BEM for the Early Stage of Unsteady Transport Process. *International Journal for Numerical Methods in Engineering*, in press.

[20] Partridge PW, Brebbia CA, Wrobel LC. The Dual Reciprocity Boundary Element Method. Southampton UK: Computational Mechanics Publications; 1992.

Bruno Natalini
Facultad de Ingeniería, Universidad Nacional del Nordeste,
Av. Las Heras 727-CP 3500 Resistencia, Provincia del Chaco, Argentina

Viktor Popov
Wessex Institute of Technology, Environmental Fluid Mechanics
Ashurst Lodge, Southampton, SO40 7AA, UK